Article

Fractional optimal control strategies for mitigating cholera epidemics: A mathematical modeling approach

Barira Afzal[1,*], Muhammad Umar Riaz[2], Mustafa Habib[1]

[1] Department of Mathematics, University of Engineering and Technology, Lahore 54890, Pakistan

[2] University of the Punjab, Lahore 54590, Pakistan

* Corresponding author: Barira Afzal, bariramalik33@gmail.com

Abstract: The SIQRB model is employed in this research to propose a Caputo-based fractional derivative optimal control model for the mitigation of cholera epidemics. Significant properties of the model, such as the non-negativity and boundedness of the solution, are verified. The basic reproduction number, $\mathcal{R}_0$, is calculated using the spectral radius of the next-generation matrix. The stability analysis demonstrates that the disease-free equilibrium is locally asymptotically stable when $\mathcal{R}_0 < 1$, while the endemic equilibrium is stable when $\mathcal{R}_0 > 1$. Numerical simulations are conducted using Euler's method to demonstrate the importance of the control function. These MATLAB-based simulations illustrate the impact of fractional-order derivatives on cholera transmission dynamics and confirm the analytical results. The efficacy of fractional optimal control approaches in mitigating cholera epidemics is demonstrated.

Keywords: cholera epidemics; mathematical modeling; fractional optimal control; caputo derivative; SIQRB model; MATLAB

1. Introduction

Cholera is a severe gastrointestinal disease caused by the comma-shaped, highly mobile bacterium Vibrio cholerae. Though there are more than 200 serogroups of the bacterium Vibrio cholerae, the disease is exclusively caused by O1 and O139. Cholera is most common in areas with poor sanitation and limited access to clean water. John Snow demonstrated in 1854 that ingesting contaminated water could lead to cholera epidemics [1]. Ingestion of contaminated food or water is the primary mode of transmission, while person-to-person contact through infected food or surfaces is the secondary mode. Cholera takes 18 h to 5 days to incubate, and symptoms start to show up nearly immediately [2]. Abdominal cramps, vomiting, diarrhea, and dehydration are typical symptoms. Cholera is still a prevalent disease across Africa and Asia, with significant outbreaks in Haiti and Zimbabwe.

Mathematical models play a crucial role in understanding the transmission dynamics of cholera and developing effective mitigation strategies. Traditional compartmental models, such as SIR, SEIR, and their extensions, have been widely used in epidemiological research. However, these integer-order models often fail to account for the memory-dependent nature of infectious disease dynamics, which is essential for accurately simulating long-term epidemics.

The study of cholera epidemic dynamics began with the seminal research of Capasso and Paveri-Fontana [3], who used a model that focused on infected individuals and free-living pathogens to examine a Mediterranean cholera outbreak.

This important research served as the basis for other models, including Codeço's [4] expansion, which included bacterial concentration in an epidemiological framework pertaining to humans and their environments. Hartley et al. [5] improved cholera modeling by adding nonlinear incidence and a hyper-infectious stage of Vibrio cholerae, and Mukandavire et al. [6], who calculated the reproduction number during the cholera epidemic in Zimbabwe. Chen et al. [7] extended these models by employing partial differential equations to study the spatial spread of cholera.

Incorporating modern techniques into cholera modeling has been the focus of recent developments. For instance, researchers in Tanzania used machine learning to forecast cholera outbreaks based on seasonal weather patterns, while Purnawan and Cahyaningtias [8] proposed optimal control strategies, such as quarantine and water sanitation.

Recent studies have demonstrated the advantages of fractional-order models in epidemiology. Unlike traditional models, fractional calculus accounts for memory effects and non-local interactions, making it particularly useful for modeling diseases such as tuberculosis, dengue, and COVID-19. The Caputo fractional derivative has been successfully applied in these contexts, offering better predictive accuracy and improved control strategies [9]. Cui et al. [10] developed a nonlinear fractional SVIR-B model, incorporating faulty vaccination and saturation treatment, further demonstrating the effectiveness of fractional approaches.

This study employs the SIQRB model to propose a Caputo-based fractional derivative optimal control framework for cholera epidemic mitigation. Unlike previous research that primarily focused on integer-order models, this study extends the analysis by incorporating fractional-order dynamics, which provide a more realistic representation of disease transmission patterns.

To determine optimal intervention strategies, we use Pontryagin's Maximum Principle, focusing on quarantine measures to minimize the number of infected individuals and bacterial concentration. Numerical simulations, based on data from the 2010 cholera outbreak in Haiti, demonstrate the superiority of fractional-order models in accurately capturing epidemic trends and optimizing control measures.

This research contributes to the growing body of literature supporting fractional optimal control models for epidemic mitigation. By integrating memory effects and optimal intervention strategies, our findings reinforce the importance of fractional calculus in modern epidemiological modeling and provide a more effective approach to controlling cholera outbreaks.

The paper is structured as follows: The preliminaries and model formulation are presented in Section 2, mathematical analysis of the fractional derivative model is presented in Section 3, the fractional optimal control problem is discussed in Section 4, and the numerical simulation results are shown in Section 5 to support the analytical conclusions. Finally, Section 6 provides a conclusion.

2. Preliminaries and model formulation

This section describes some preliminary fractional calculus and fractional-order differential equations for the cholera model.

2.1. Preliminaries

Fractional calculus extends an adaptable framework for modeling complex systems by extending the ideas of integrals and derivatives to non-integer orders. Riemann-Liouville fractional integral and derivative and Caputo fractional derivative are common fractional operators used in mathematical modeling and engineering applications. The following are important definitions:

Definition 1. *Left Riemann-Liouville fractional integral $_a^L D_t^{-\alpha} f$ of order $\alpha \in R^+$ is defined by*

$$_a^L D_t^{-\alpha} f(t) = \frac{1}{\Gamma(\alpha)} \int_a^t (t-s)^{\alpha-1} f(s) ds, t\epsilon[a,b].$$

Definition 2. *Right Riemann-Liouville fractional integral $_t^R D_b^{-\alpha} f$ of order $\alpha \in R^+$ is defined by*

$$_t^R D_b^{-\alpha} f(t) = \frac{1}{\Gamma(\alpha)} \int_t^b (s-t)^{\alpha-1} f(s) ds, t\epsilon[a,b].$$

Definition 3. *Left Riemann-Liouville fractional derivative of order α is defined by*

$$_a^L D_x^{\alpha} [f(x)] = \frac{1}{\Gamma(n-\alpha)} \left(\frac{d}{dx}\right)^n \int_a^x (x-t)^{n-1-\alpha} f(t) dt, \epsilon[a,b].$$

Definition 4. *Right Riemann-Liouville fractional derivative of order α is defined by*

$$_t^R D_b^{\alpha} [f(x)] = \frac{1}{\Gamma(n-\alpha)} \left(-\frac{d}{dx}\right)^n \int_x^b (t-x)^{n-1-\alpha} f(t) dt, x\epsilon[a,b].$$

Definition 5. *Left Caputo fractional derivative of order α is defined by*

$$_a^C D_x^{\alpha} [f(x)] = \frac{1}{\Gamma(n-\alpha)} \left(\frac{d}{dx}\right)^n \int_a^x (x-t)^{n-1-\alpha} f(t) dt, x \epsilon[a,b].$$

Definition 6. *Right Caputo fractional derivative of order α is defined by*

$$_t^C D_b^{\alpha} [f(x)] = \frac{1}{\Gamma(n-\alpha)} \left(-\frac{d}{dx}\right)^n \int_x^b (t-x)^{n-1-\alpha} f(t) dt, x\epsilon[a,b],$$

where Γ is a gamma function.

Definition 7. *The Laplace transform of Caputo fractional derivative is defined as*

$$L\{_0^C D_t^{\alpha} f(t)\} = \lambda^{\alpha} F(\lambda) - \sum_{k=0}^{n-1} \lambda^{\alpha-k-1} f^k(0),$$

with $F(\lambda)$ the Laplace transform of $f(t)$.

Definition 8. *The Mittag-Leffler function with two parameters for any complex number z is defined as*

$$E_{\alpha,\beta}(z) = \sum_{k=0}^{\infty} \frac{z^k}{\Gamma(\alpha k+\beta)}, \alpha, \beta > 0.$$

where Γ is a gamma function.

Corollary 1. *Corollary of Gershgorin's Circle Theorem: Let B be an $n \times n$ matrix with real entries. If the diagonal elements a_{ii} of B satisfy*

$$a_{ii} < -r_i,$$

where

$$r_i = \sum_{j=1, j\neq i}^n |a_{ij}|,$$

For $i = 1, 2, 3, \ldots, n$, *then the eigenvalues of B are negative or have negative real parts* [11].

2.2. Model formulation

In this section, we provide a deterministic mathematical model with cholera control strategies that are optimal. Following the SIQR (Susceptible–Infected–Quarantined–Recovered) framework, the model concentrates on the dynamics of bacterial concentration. There are four compartments in the total population $N(t)$: Susceptible $S(t)$, Infected $I(t)$, Quarantined $Q(t)$ and Recovered $R(t)$. Furthermore, the bacterial concentration is represented by $B(t)$. Additionally, the model is formulated with the following assumptions:

i)   The model takes into account a positive recruitment rate Λ into the susceptible class $S(t)$.

ii) A positive natural death rate is μ.

iii) The rate at which susceptible individuals get cholera is $\frac{\beta B}{\kappa + B}$, where $\beta > 0$ represents the rate at which bacteria are ingested.

iv) κ represents the half-saturation constant.

v) β represents contact with contaminated materials.

vi) Recovered individuals become susceptible again when their immunity loses at a rate of ω.

vii) Quarantined and treated at a rate of δ.

viii) Infected individuals recover at a rate of ε.

ix) The mortality rates associated with disease are α_1 for infected individuals.

x)   The mortality rates associated with disease are α_2 for quarantined individuals.

xi) The rate at which each infected individual increases the concentration of bacteria is η.

xii) The rate at which bacteria die is d.

The following block diagram, in general, describes the dynamics of the human population susceptible to cholera epidemics and the specified assumptions.

The mathematical model of the cholera epidemic with optimal control strategies is based on model assumptions and **Figure 1**.

$$\begin{cases} S(t) = \Lambda - \left(\dfrac{\beta B(t)}{\kappa + B(t)} - \mu \right) S(t) + \omega R(t) \\[2mm] I(t) = \dfrac{\beta B(t)}{\kappa + B(t)} S(t) - \delta u(t) I(t) - (\alpha_1 + \mu) I(t) \\[2mm] Q(t) = \delta u(t) I(t) - (\varepsilon + \alpha_2 + \mu) Q(t) \\[2mm] R(t) = \varepsilon Q(t) - (\omega + \mu) R(t) \\[2mm] B(t) = \eta I(t) - d B(t) \end{cases} \tag{1}$$

with non-negative initial conditions:

$$S(0) \geq 0, I(0) \geq 0, Q(0) \geq 0, R(0) \geq 0 \ and \ B(0) \geq 0.$$
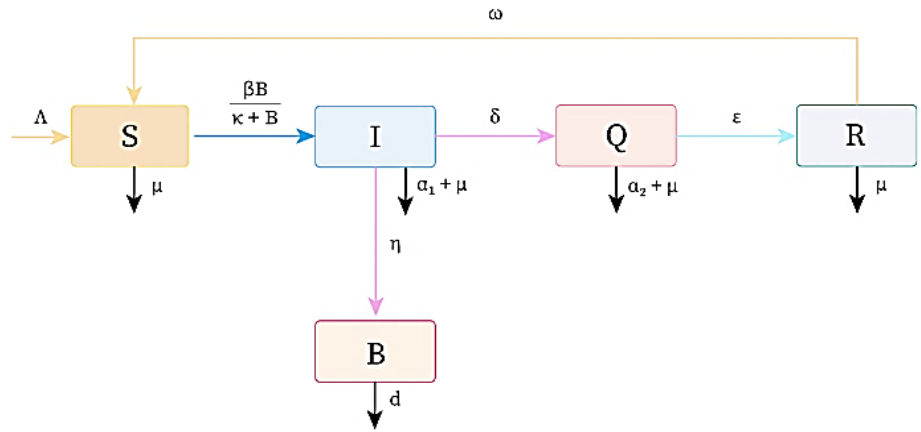
Figure 1. Block diagram of the cholera model.

2.3. System of fractional order differential equations

The following system of nonlinear equations defines the dynamics of the cholera epidemic in this study using the Caputo fractional derivative of order α and $0 < \alpha \leq 1$:

$$
\begin{cases}
{}_{0}^{C}D_t^{\alpha}S(t) = \Lambda - \left(\dfrac{\beta B(t)}{\kappa + B(t)} - \mu\right)S(t) + \omega R(t) \\[2mm]
{}_{0}^{C}D_t^{\alpha}I(t) = \dfrac{\beta B(t)}{\kappa + B(t)}S(t) - (\delta + \alpha_1 + \mu)I(t) \\[2mm]
{}_{0}^{C}D_t^{\alpha}Q(t) = \delta I(t) - (\varepsilon + \alpha_2 + \mu)Q(t) \\[2mm]
{}_{0}^{C}D_t^{\alpha}R(t) = \varepsilon Q(t) - (\omega + \mu)R(t) \\[2mm]
{}_{0}^{C}D_t^{\alpha}B(t) = \eta I(t) - dB(t)
\end{cases}
\tag{2}
$$

with non-negative initial conditions subject to

$$S(0) \geq 0, I(0) \geq 0, Q(0) \geq 0, R(0) \geq 0, B(0) \geq 0.$$

3. Mathematical analysis of fractional derivative model

This section demonstrates the mathematical and biological viability of the fractional order derivative cholera model. This involves determining the non-negativity and boundedness of the solution.

3.1. Non-negativity and boundedness of solution

Non-negativity of a solution means the population thrives; however, boundedness is the characteristic of population growth that is inherently constrained by limiting resources. First, we show that the solution of the system is always non-negative. From model (2), we have

$$\left.{}_{0}^{C}D_t^{\alpha}S(t)\right|_{S=0} = \Lambda + \omega R(t) > 0,$$

$$\left.{}_{0}^{C}D_t^{\alpha}I(t)\right|_{I=0} = \frac{\beta B(t)}{\kappa + B(t)}S(t) > 0,$$

$$\left.{}_{0}^{C}D_t^{\alpha}Q(t)\right|_{Q=0} = \delta I(t) > 0,$$

$$\left.{}_{0}^{C}D_t^{\alpha}R(t)\right|_{R=0} = \varepsilon Q(t) > 0,$$

$$\left.{}_0^C D_t^\alpha B(t)\right|_{B=0} = \eta I(t) > 0.$$

Hence, model (2) has a non-negative solution [12].

Next, we note that the two components that determine the boundedness of the solution are the number of humans in the community and its bacterial concentration. Consider

$$N(t) = S(t) + I(t) + Q(t) + R(t).$$

For the human population, the first four equations of system (2) are added up to give

$${}_0^C D_t^\alpha N(t) = {}_0^C D_t^\alpha S(t) + {}_0^C D_t^\alpha I(t) + {}_0^C D_t^\alpha Q(t) + {}_0^C D_t^\alpha R(t).$$

We get

$${}_0^C D_t^\alpha N(t) = \Lambda - \mu N(t) - \alpha_1 I(t) - \alpha_2 Q(t).$$

In the absence of infection, there is no quarantine. Thus

$${}_0^C D_t^\alpha N(t) \leq \Lambda - \mu N(t).$$

Applying the Laplace transform method, we solve the inequality with the initial condition $N(t_0) \geq 0$ to find

$$\mathrm{L}\{{}_0^C D_t^\alpha N(t)\}(s) \leq \mathrm{L}\{\Lambda\}(s) - \mu \mathrm{L}\{N(t)\}(s).$$

We get

$$s^\alpha N(s) - \sum_{k=0}^{n-1} s^{\alpha-1-k} N^k(t_0) \leq \frac{\Lambda}{s} - \mu N(s),$$

where $\mathrm{L}\{N(t)\}(s) = N(s)$.

$$N(s)(s^\alpha + \mu) \leq \frac{\Lambda}{s} + \sum_{k=0}^{n-1} s^{\alpha-1-k} N^k(t_0),$$

$$N(s) \leq \frac{\Lambda}{s(s^\alpha + \mu)} + \frac{\sum_{k=0}^{n-1} s^{\alpha-1-k} N^k(t_0)}{(s^\alpha + \mu)}.$$

Now we apply the inverse Laplace transform

$$\mathrm{L}^{-1}\{N(s)\} \leq \mathrm{L}^{-1} \frac{\Lambda}{s(s^\alpha + \mu)} + \sum_{k=0}^{n-1} N^k(t_0)\, \mathrm{L}^{-1} \frac{s^{\alpha-1-k}}{(s^\alpha + \mu)},$$

$$N(t) \leq \Lambda t^\alpha E_{\alpha,\alpha+1}(-\mu t^\alpha) + \sum_{k=0}^{n-1} N^k(t_0)\, t^{\alpha-1-k} E_{\alpha,\alpha-k}(-\mu t^\alpha),$$

where $E_{\alpha,\beta}(z) = \sum_{k=0}^\infty \frac{z^k}{\Gamma(\alpha k + \beta)}$ is Mittag–Leffler function with parameters α and β.

The Mittag-Leffler functions of the fractional differential equation decay to zero as $t \to \infty$, which causes $N(t)$ to asymptotically approach and stabilize at the upper bound $\frac{\Lambda}{\mu}$. It may be concluded that $N(t) \leq \frac{\Lambda}{\mu}$.

For the concentration of bacteria, it follows that

$${}_0^C D_t^\alpha B(t) = \eta I(t) - d B(t) \leq \eta \frac{\Lambda}{\mu} - d B(t).$$

Then we have

$$B(t) \leq \frac{\Lambda \eta}{\mu d}.$$

The analysis and discussion described above prove that the solutions of the system remain bounded.

3.2. Equilibrium points and stability analysis

To obtain the equilibrium points, we set all time fractional derivatives in the system of Equation (2) to zero and solve simultaneously. i.e.,

$$_0^C D_t^\alpha S(t) = {}_0^C D_t^\alpha I(t) = {}_0^C D_t^\alpha Q(t) = {}_0^C D_t^\alpha R(t) = {}_0^C D_t^\alpha B(t) = 0.$$

There are two equilibrium points:

Disease-free equilibrium point: A disease-free equilibrium (DFE) point in a cholera model is a steady state without Vibrio cholera ($I = 0$). So, DFE point (E^0) is given by

$$E^0 = (S^0, I^0, Q^0, R^0, B^0) = \left(\frac{\Lambda}{\mu}, 0, 0, 0, 0\right).$$

Endemic equilibrium point: Equilibrium points are deemed endemic when the disease continues to spread throughout the population ($I \neq 0$). Then the endemic equilibrium point (E^*) is given as:

$$E^* = (S^*, I^*, Q^*, R^*, B^*).$$

where

$$S^* = \frac{k_1 \mathrm{e}}{\eta \mathfrak{D}},$$

$$I^* = \frac{\beta \Lambda k_2 k_3}{\mathcal{R}_0 \mathfrak{D}} (\mathcal{R}_0 - 1),$$

$$Q^* = \frac{\beta \Lambda \delta k_3}{\mathcal{R}_0 \mathfrak{D}} (\mathcal{R}_0 - 1),$$

$$R^* = \frac{\beta \Lambda \delta \varepsilon}{\mathcal{R}_0 \mathfrak{D}} (\mathcal{R}_0 - 1),$$

$$B^* = \frac{\beta \Lambda \eta k_2 k_3}{\mathcal{R}_0 \mathfrak{D} d} (\mathcal{R}_0 - 1),$$

where $\mathrm{e} = \Lambda \eta k_2 k_3 + \kappa d(k_1 k_2 k_3 - \delta \omega \varepsilon)$, $k_1 = \delta + \alpha_1 + \mu$, $k_2 = \varepsilon + \alpha_2 + \mu$, $k_3 = \omega + \mu$, and $\mathfrak{D} = k_1 k_2 k_3 \mu + k_1 k_2 k_3 \beta - \beta \delta \omega \varepsilon$.

3.3. Basic reproduction number ($\mathcal{R}_0$)

One of the most significant quantities in epidemiology is the basic reproduction number ($\mathcal{R}_0$). It is defined as the average number of secondary infections that occur when an infected individual comes into a host group where every individual is susceptible. To calculate ($\mathcal{R}_0$), we use the next-generation matrix approach explained in [13]. Mathematically, ($\mathcal{R}_0$) is the spectral radius of the product matrix. i.e.,

$$\mathcal{R}_0 = \rho(F_0 V_0^{-1}) = \frac{\beta \Lambda \eta}{\kappa \mu d k_1},$$

where ρ denotes the spectral radius.

3.4. Stability analysis of equilibrium points

To determine the stability analysis of equilibrium points, we compute the Jacobian matrix $J(s)$, which is obtained from system (2) and is given as

$$J(s) = \begin{bmatrix} -\frac{\beta B(t)}{\kappa+B} - \mu & 0 & 0 & \omega & -\frac{\beta \kappa S(t)}{(\kappa+B(t))^2} \\ \frac{\beta B(t)}{\kappa+B} & -k_1 & 0 & 0 & \frac{\beta \kappa S(t)}{(\kappa+B(t))^2} \\ 0 & \delta & -k_2 & 0 & 0 \\ 0 & 0 & \varepsilon & -k_3 & 0 \\ 0 & \eta & 0 & 0 & -d \end{bmatrix}.$$

3.5. Local stability for the disease-free equilibrium

Theorem. *The disease-free equilibrium* (E^0) *is locally asymptotically stable if* $\mathcal{R}_0 < 1$.

Proof. To analyze the local behavior of each equilibrium point, corollary of Gershgorin's Circle Theorem is used to calculate the Jacobian matrix $J(s)$ at the equilibrium point E^0.

Substituting the disease-free equilibrium point $E^0 = \left(\frac{\Lambda}{\mu}, 0,0,0,0\right)$ into the Jacobian matrix $J(s)$, we get

$$J(E^0) = \begin{bmatrix} -\mu & 0 & 0 & \omega & -\frac{\beta \Lambda}{\mu\kappa} \\ 0 & -k_1 & 0 & 0 & \frac{\beta \Lambda}{\mu\kappa} \\ 0 & \delta & -k_2 & 0 & 0 \\ 0 & 0 & \varepsilon & -k_3 & 0 \\ 0 & \eta & 0 & 0 & -d \end{bmatrix}.$$

The eigenvalues $\lambda = -\mu$, $\lambda = -k_3$ and $\lambda = -k_2$ are obtained sequentially by expansions and reductions along the first, third, and second columns, respectively, by matrix expansion. Finally, we have sub-matrix

$$J(E^0) = \begin{bmatrix} -k_1 & \frac{\beta \Lambda}{\mu\kappa} \\ \eta & -d \end{bmatrix}.$$

Matrix $J(E^0)$ satisfies the corollary of Gershgorin's Circle theorem if the following inequalities hold;

$$k_1 > \frac{\beta \Lambda}{\mu\kappa} \tag{3}$$

$$d > \eta \tag{4}$$

Combining Equations (3) and (4)

$$k_1 d > \frac{\beta \Lambda \eta}{\mu\kappa},$$

$$1 > \frac{\beta \Lambda \eta}{\kappa \mu d k_1} = \mathcal{R}_0,$$

$$\mathcal{R}_0 < 1,$$

Hence, disease-free equilibrium point is locally asymptotically stable since $\mathcal{R}_0 < 1$ [14]. □

3.6. Local stability for the endemic equilibrium

Theorem. *The endemic equilibrium* (E^*) *is locally asymptotically stable if* $\mathcal{R}_0 > 1$.

Proof. Eigenvalues of the Jacobian matrix $J(s)$ must have negative real part for the endemic equilibrium to be asymptotically stable. At endemic equilibrium point (E^*), the Jacobian matrix is:

$$J(E^*) = \begin{bmatrix} -\frac{\beta B^*(t)}{\kappa + B^*(t)} - \mu & 0 & 0 & \omega & -\frac{\beta \kappa S^*(t)}{(\kappa + B^*(t))^2} \\ \frac{\beta B^*(t)}{\kappa + B^*(t)} & -k_1 & 0 & 0 & \frac{\beta \kappa S^*(t)}{(\kappa + B^*(t))^2} \\ 0 & \delta & -k_2 & 0 & 0 \\ 0 & 0 & \varepsilon & -k_3 & 0 \\ 0 & \eta & 0 & 0 & -d \end{bmatrix}.$$

Consider $X = \frac{\beta B^*(t)}{\kappa + B^*(t)}$ and $Y = \frac{\beta \kappa S^*(t)}{(\kappa + B^*(t))^2}$. Then

$$J(E^*) = \begin{bmatrix} -X - \mu & 0 & 0 & \omega & -Y \\ X & -k_1 & 0 & 0 & Y \\ 0 & \delta & -k_2 & 0 & 0 \\ 0 & 0 & \varepsilon & -k_3 & 0 \\ 0 & \eta & 0 & 0 & -d \end{bmatrix}.$$

Following Jacobian matrix is obtained by elementary row operations and simplification:

$$J(E^*) = \begin{bmatrix} -Z_1 & 0 & 0 & \omega & -Y \\ 0 & -Z_1 k_1 & 0 & \omega X & \mu Y \\ 0 & 0 & -Z_1 k_1 k_2 & \delta \omega X & \delta \mu Y \\ 0 & 0 & 0 & -(Z_2 - Z_3) & \delta \varepsilon \mu Y \\ 0 & 0 & 0 & 0 & -[d(-Z_2 + Z_3) + Z_4] \end{bmatrix},$$

where

$$Z_1 = X + \mu,$$

$$Z_2 = Z_1 k_1 k_2 k_3,$$

$$Z_3 = \delta \varepsilon \omega X,$$

$$Z_4 = k_2 k_3 \eta \mu Y.$$

The characteristic polynomial of the Jacobian matrix $J(E^*)$ is

$$p(E^*) = det(\lambda I - J(E^*)) = 0,$$

$$(\lambda + Z_1)(\lambda + Z_1 k_1)(\lambda + Z_1 k_1 k_2)\big(\lambda + (Z_2 - Z_3)\big)(\lambda + d(-Z_2 + Z_3) + Z_4) = 0.$$

that is,

$$\lambda_1 = -Z_1 = -(X + \mu) < 0,$$

$$\lambda_2 = -Z_1 k_1 = -k_1(X + \mu) < 0,$$

$$\lambda_3 = -Z_1 k_1 k_2 = -k_1 k_2(X + \mu) < 0,$$

$$\lambda_4 = -(Z_2 - Z_3) = -(Z_1 k_1 k_2 k_3 - \delta\varepsilon\omega X) = -(k_1 k_2 k_3(X + \mu) - \delta\varepsilon\omega X) < 0,$$

$$-k_1 k_2 k_3 X - k_1 k_2 k_3 \mu + \delta\varepsilon\omega X < 0,$$

$$(-k_1 k_2 k_3 + \delta\varepsilon\omega)\frac{\beta B^*(t)}{\kappa + B^*(t)} - k_1 k_2 k_3 \mu < 0,$$

$$(-k_1 k_2 k_3 + \delta\varepsilon\omega)\frac{\beta\eta I^*}{\kappa d + \eta I^*} < k_1 k_2 k_3 \mu,$$

$$-\mathfrak{D}\eta\left(\frac{\beta\Lambda k_2 k_3}{\mathcal{R}_0 \mathfrak{D}}(\mathcal{R}_0 - 1)\right) - k_1 k_2 k_3 \mu\kappa d < 0,$$

$$\lambda_4 = -\frac{\beta\Lambda\eta}{\mathcal{R}_0}(\mathcal{R}_0 - 1) - k_1 \mu\kappa d < 0,$$

If $\mathcal{R}_0 > 1$ then $\lambda_4 < 0$.

$$\lambda_5 = -(d(-Z_2 + Z_3) + Z_4) = -d\lambda_4 - k_2 k_3 \eta\mu Y < 0.$$

Since $\lambda_4 < 0$ then λ_5 will also be less than zero.

By Routh Hurwitz's criterion, all eigenvalues of $J(E^*)$ have negative real part. Therefore, the endemic equilibrium E^* of the model is locally asymptotically stable if $\mathcal{R}_0 > 1$ [15]. □

4. Fractional optimal control problem

In this section, a fractional optimal control function $u(t)$, representing the fraction of infected individuals treated and quarantined, is added to model (2) to develop strategies to minimize the cholera epidemic. Strict quarantine without optimization could result in economic disruptions, resource constraints, and social resistance. Increasing quarantine only proportionate to infection rates assumes an ideal scenario where enforcement and compliance are unlimited, which is unrealistic. The fractional optimal control approach balances disease mitigation with feasible intervention efforts, requiring the mathematical sophistication required for real-world applicability. Therefore, a control variable is necessary because quarantining everyone is neither practical nor cost-effective.

The control variable $u(t)$, restricted to the closed interval $[0, 1]$, optimizes intervention strategies to reduce cholera transmission. System (2) is modified as follows by adding this control:

$$\begin{cases} {}_0^C D_t^\alpha S(t) = \Lambda - \left(\frac{\beta B(t)}{\kappa + B(t)} + \mu\right)S(t) + \omega R(t) \\ {}_0^C D_t^\alpha I(t) = \frac{\beta B(t)}{\kappa + B(t)}S(t) - \delta u(t)I(t) - (\alpha_1 + \mu)I(t) \\ {}_0^C D_t^\alpha Q(t) = \delta u(t)I(t) - (\varepsilon + \alpha_2 + \mu)Q(t) \\ {}_0^C D_t^\alpha R(t) = \varepsilon Q(t) - (\omega + \mu)R(t) \\ {}_0^C D_t^\alpha B(t) = \eta I(t) - dB(t) \end{cases} \tag{5}$$

The non-negative initial condition in this case is

$$S(0) = S_0, I(0) = I_0, Q(0) = Q_0, R(0) = R_0, B(0) = B_0.$$

The set of admissible trajectories, denoted by $\wp$, is defined as

$$\wp = \{X(\cdot)\epsilon C^{1,1}([0,T];\mathbb{R}^5)\},$$

where $X = (S, I, Q, R, B)$ and the control set U is defined as

$$U = \{u \text{ is Lebsegue measurable } ([0,T];\mathbb{R})|0 \le u(t) \le 1, \forall t\epsilon[0,T]\}.$$

Our goal is to reduce the number of infected people and the presence of bacteria while simultaneously minimizing the cost of control measures like quarantine. Our model incorporates an intervention cost function into the optimal control framework, which not only shows the effectiveness of quarantine but also quantifies its impact. For a given time T, the cost of intervention is factored in through an objective functional, typically formulated as:

$$J(u) = \int_0^T \left(I + B + \frac{1}{2}Cu^2\right)dt,$$

where C is a positive constant. Our goal is to find the optimal solution $u^*\epsilon U$ to control system (3) and achieve the minimum value for the objective function, i.e.,

$$J(u^*) = min \int_0^T \left(I + B + \frac{1}{2}Cu^2\right)dt.$$

According to Pontryagin's maximum principle, if u^* is the optimal solution for the objective functional, then there exists an adjoint vector $\lambda(t) = \left(\lambda_S,\ \lambda_I,\ \lambda_Q,\ \lambda_R,\ \lambda_B\right)\epsilon\mathbb{R}_+^5$ that satisfies the following conditions:

(i) The control system is

$$_0^C D_t^\alpha S(t) = \frac{\partial H}{\partial \lambda_S}(t), {}_0^C D_t^\alpha I(t) = \frac{\partial H}{\partial \lambda_I}(t), {}_0^C D_t^\alpha Q(t) = \frac{\partial H}{\partial \lambda_Q}(t),$$

$$_0^C D_t^\alpha R(t) = \frac{\partial H}{\partial \lambda_R}(t), {}_0^C D_t^\alpha B(t) = \frac{\partial H}{\partial \lambda_B}(t).$$

(ii) The co-state system is

$$_0^C D_t^\alpha \lambda_S = -\frac{\partial H}{\partial S}, {}_0^C D_t^\alpha \lambda_I = -\frac{\partial H}{\partial I}, {}_0^C D_t^\alpha \lambda_Q = -\frac{\partial H}{\partial Q},$$

$$_0^C D_t^\alpha \lambda_R = -\frac{\partial H}{\partial R}, {}_0^C D_t^\alpha \lambda_B = -\frac{\partial H}{\partial B}.$$

(iii) The stationary condition is

$$\frac{\partial H}{\partial u} = 0.$$

(iv) The transversality conditions are

$$\lambda_S(T) = 0, \lambda_I(T) = 0, \lambda_Q(T) = 0, \lambda_R(T) = 0, \lambda_B(T) = 0.$$

and the Hamiltonian function is defined as

$$H(t,X,u,\lambda) = L(I,B,u) + \lambda_S\left(\Lambda - \left(\frac{\beta B(t)}{\kappa + B(t)} + \mu\right)S(t) + \omega R(t)\right) + \lambda_I\left(\frac{\beta B(t)}{\kappa + B}S(t) - \delta u(t)I(t) - (\alpha_1 + \mu)I(t)\right) +$$

$$\lambda_Q\left(\delta u(t)I(t) - (\varepsilon + \alpha_2 + \mu)Q(t)\right) + \lambda_R\left(\varepsilon Q(t) - (\omega + \mu)R(t)\right) + \lambda_B\left(\eta I(t) - dB(t)\right),$$

where $\lambda_S(t), \lambda_I(t), \lambda_Q(t), \lambda_R(t)$ and $\lambda_B(t)$ are adjoint variables or co-state variables. Calculating the partial derivatives of the Hamiltonian $H(t,X,u,\lambda)$ with respect to the related state variable yields the system solution.

Theorem. *The optimal control of model (3) is such that the associated variables satisfy the following equation and the objective function on U is minimal.*

$$\begin{cases} {}^{C}_{0}D^{\alpha}_{t}\lambda_{S}(t) = \lambda_{S}\left(\dfrac{\beta B(t)}{\kappa + B(t)} + \mu\right) - \lambda_{I}\left(\dfrac{\beta B(t)}{\kappa + B(t)}\right) \\ {}^{C}_{0}D^{\alpha}_{t}\lambda_{I}(t) = -1 + \lambda_{I}(\delta u^{*}(t) + \alpha_{1} + \mu) - \lambda_{Q}\delta u^{*}(t) - \lambda_{B}\eta \\ {}^{C}_{0}D^{\alpha}_{t}\lambda_{Q}(t) = \lambda_{Q}(\varepsilon + \alpha_{2} + \mu) - \lambda_{R}\varepsilon \\ {}^{C}_{0}D^{\alpha}_{t}\lambda_{R}(t) = -\lambda_{S}\omega + \lambda_{R}(\omega + \mu) \\ {}^{C}_{0}D^{\alpha}_{t}\lambda_{B}(t) = -1 + \lambda_{S}\dfrac{\beta\kappa S(t)}{\left(\kappa + B(t)\right)^{2}} - \lambda_{I}\dfrac{\beta\kappa S(t)}{\left(\kappa + B(t)\right)^{2}} + \lambda_{B}d \end{cases} \quad (6)$$

with transversality conditions

$$\lambda_{S}(T) = 0, \lambda_{I}(T) = 0, \lambda_{Q}(T) = 0, \lambda_{R}(T) = 0, \lambda_{B}(T) = 0.$$

Additionally, the optimal control u^{*} can be expressed as

$$u^{*}(t) = \min\left\{\max\left\{0, \dfrac{\delta I(t)\left(\lambda_{I}(t) - \lambda_{Q}(t)\right)}{c}\right\}, 1\right\}.$$

Proof. The adjoint equation and transversal condition can be obtained by applying the Pontryagin Maximum Principle [16].

$$\begin{aligned} {}^{C}_{0}D^{\alpha}_{t}\lambda_{S}(t) &= -\frac{\partial H}{\partial S} = \lambda_{S}\left(\frac{\beta B(t)}{\kappa + B(t)} + \mu\right) - \lambda_{I}\left(\frac{\beta B(t)}{\kappa + B(t)}\right), \end{aligned}$$

$$\begin{aligned} {}^{C}_{0}D^{\alpha}_{t}\lambda_{I}(t) &= -\frac{\partial H}{\partial I} = -1 + \lambda_{I}(\delta u^{*}(t) + \alpha_{1} + \mu) - \lambda_{Q}\delta u^{*}(t) - \lambda_{B}\eta, \end{aligned}$$

$$\begin{aligned} {}^{C}_{0}D^{\alpha}_{t}\lambda_{Q}(t) &= -\frac{\partial H}{\partial Q} = \lambda_{Q}(\varepsilon + \alpha_{2} + \mu) - \lambda_{R}\varepsilon, \end{aligned}$$

$$\begin{aligned} {}^{C}_{0}D^{\alpha}_{t}\lambda_{R}(t) &= -\frac{\partial H}{\partial R} = -\lambda_{S}\omega + \lambda_{R}(\omega + \mu), \end{aligned}$$

$$\begin{aligned} {}^{C}_{0}D^{\alpha}_{t}\lambda_{B}(t) &= -\frac{\partial H}{\partial B} = -1 + \lambda_{S}\frac{\beta\kappa S(t)}{\left(\kappa + B(t)\right)^{2}} - \lambda_{I}\frac{\beta\kappa S(t)}{\left(\kappa + B(t)\right)^{2}} + \lambda_{B}d. \end{aligned}$$

Initial conditions are

$$S(0) = S_{0}, I(0) = I_{0}, Q(0) = Q_{0}, R(0) = R_{0}, B(0) = B_{0}.$$

Solve the following equations to get the characteristic equation of optimal control (u^{*}).

$$\frac{\partial H}{\partial u} = Cu^{*} + \delta I(t)\left(\lambda_{Q}(t) - \lambda_{I}(t)\right) = 0.$$

Therefore

$$u^{*} = \frac{\delta I(t)\left(\lambda_{I}(t) - \lambda_{Q}(t)\right)}{c}.$$

Considering the boundedness of control u, the optimal control solution u^{*} can be expressed as

$$u^{*}(t) = \min\left\{\max\left\{0, \frac{\delta I(t)\left(\lambda_{I}(t) - \lambda_{Q}(t)\right)}{c}\right\}, 1\right\}.$$

Further, the fractional optimal control u^* are obtained by partial differentiation of the Hamiltonian H with respect to u.

$$u^*(t) = \frac{\partial H}{\partial u} = \frac{\delta I(t)\left(\lambda_I(t) - \lambda_Q(t)\right)}{C}. \quad \square$$

5. Numerical simulations

The generalized Euler method is employed to determine the optimality framework of fractional-order differential problems, such as the state and adjoint equations. The analysis of the cholera model requires the following initial conditions and model parameter values:

The fractional optimal control framework states that the number of infected individuals as well as the concentration of bacteria in the environment can be considerably reduced by putting strategies like quarantine treatment into place.

The MATLAB simulations describe the dynamics of the SIQRB model using the parameters and initial conditions in **Table 1**, with $C = 2000$ and final time $T = 182$ days.

Table 1. Parameter values and initial conditions.

Parameters	Values	References
Λ	$24.4N(0)/365\,000\,(day^{-1})$	[17]
μ	$2.2493 \times 10^{-5}\,(day^{-1})$	[18]
β	$0.8\,(day^{-1})$	[19]
κ	$10^6\,(\text{cell/mL})$	[20]
ω	$0.4/365\,(day^{-1})$	[21]
ε	$0.2\,(day^{-1})$	[22]
δ	$0.05\,(day^{-1})$	Assumed
α_1	$0.015\,(day^{-1})$	[22]
α_2	$0.0001\,(day^{-1})$	[22]
η	$10\,(\text{cell/ml}\ day^{-1}\ person^{-1})$	[19]
d	$0.33\,(day^{-1})$	[19]
$S(0)$	$5750\,(\text{person})$	Assumed
$I(0)$	$1700\,(\text{person})$	[23]
$Q(0)$	$0\,(\text{person})$	Assumed
$R(0)$	$0\,(\text{person})$	Assumed
$B(0)$	$275 \times 10^3\,(\text{cell/mL})$	Assumed

The sub-model is expressed as follows to compare the simulation results for bacterial concentration and cholera-infected individuals with and without control:

$$\begin{cases} S'(t) = \Lambda - \left(\dfrac{\beta B(t)}{\kappa + B(t)} + \mu\right) S(t) \\ I'(t) = \dfrac{\beta B(t)}{\kappa + B} S(t) - (\alpha_1 + \mu) I(t) \\ B'(t) = \eta I(t) - dB(t) \end{cases} \tag{7}$$

This simplified model represents cholera dynamics without optimal control and quarantine measures, assuming that

$$\omega = \delta = \varepsilon = \alpha_2 = Q(0) = R(0) = 0.$$

The cholera epidemic in the Artibonite region is accurately described by the sub-model using the parameter values listed in **Table 1**. Simulations show that implementing a control method considerably reduces the concentration of bacteria and infectious individuals (see **Figures 2–4**).
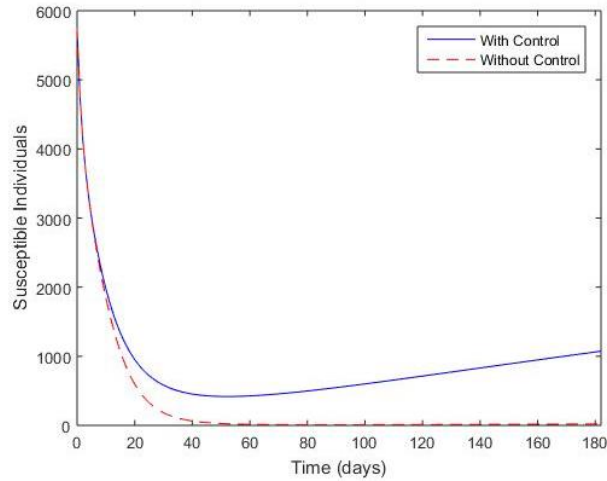
Figure 2. Optimal solutions for susceptible individuals with and without control.
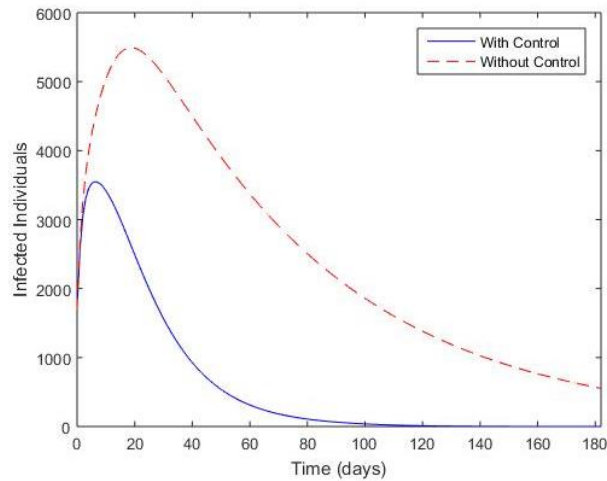
Figure 3. Optimal solutions for infected individuals, with and without control.
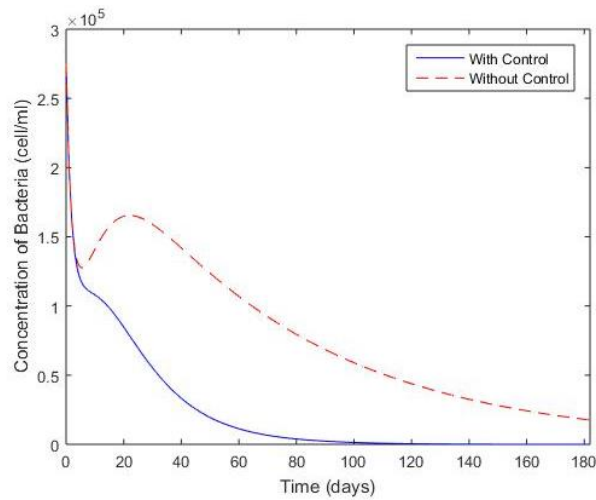
Figure 4. Optimal solutions for concentration of bacteria, with and without control.

In **Figures 5–9**, the function of fractional derivatives (α) in the dynamics of cholera is analyzed. The findings highlight memory effects (the influence of past states or events on the current behavior or dynamics of a system) importance and how they affect different subpopulations:

Because of improved immunity or more successful management mechanisms, decreased values of α, which highlight memory effects, cause the susceptible population to diminish more slowly.

As α declines, disease transmission slows down and eventually fewer people become sick.

Those under quarantine are more numerous when the values of α are higher, indicating stricter quarantine regulations. More immunity or a more successful recovery process is indicated by a lower α value, which over time leads to a bigger recovered population. Vibrio cholerae growth can be inhibited by the memory effect, which is affected by α. The concentration of bacteria in the environment is significantly reduced by higher values of α.
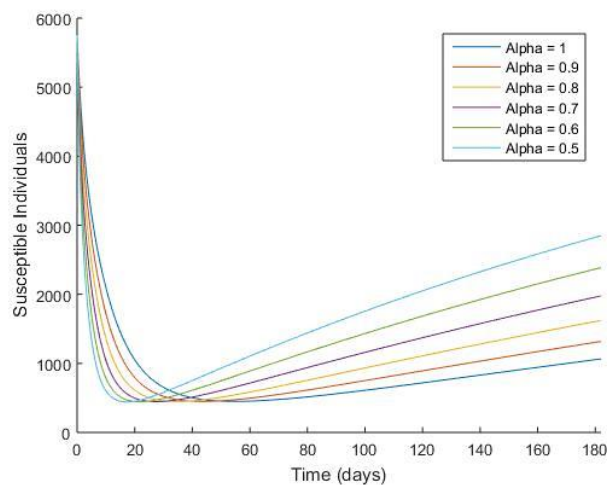
Figure 5. Simulations of susceptible individuals with different values of alpha.
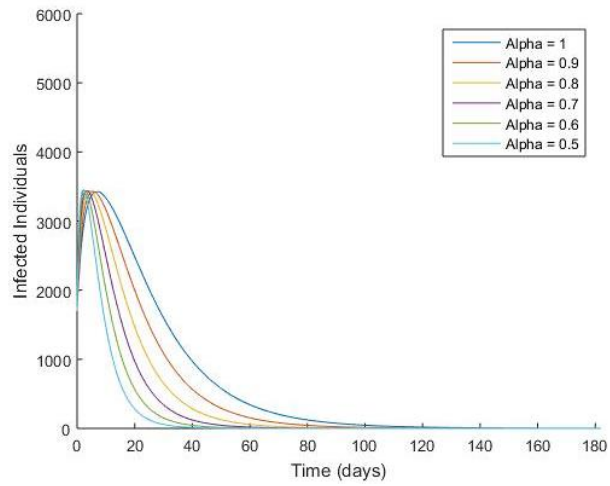
Figure 6. Simulations of infected individuals with different values of alpha.
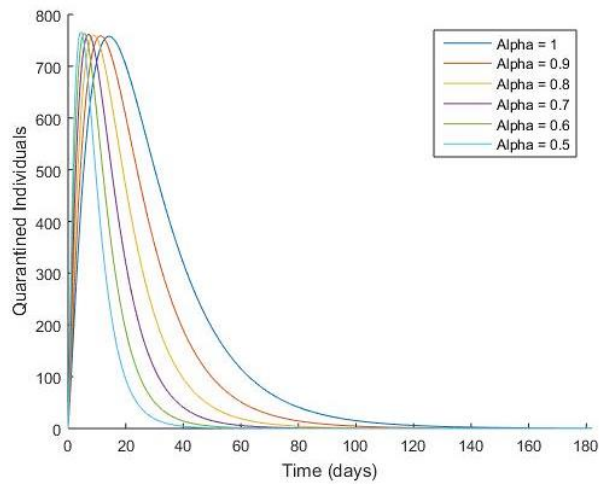
Figure 7. Simulations of quarantined individuals with different values of alpha.
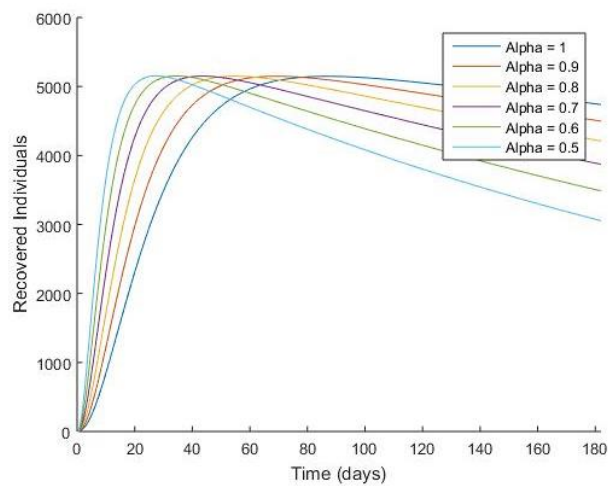
Figure 8. Simulations of recovered individuals with different values of alpha.
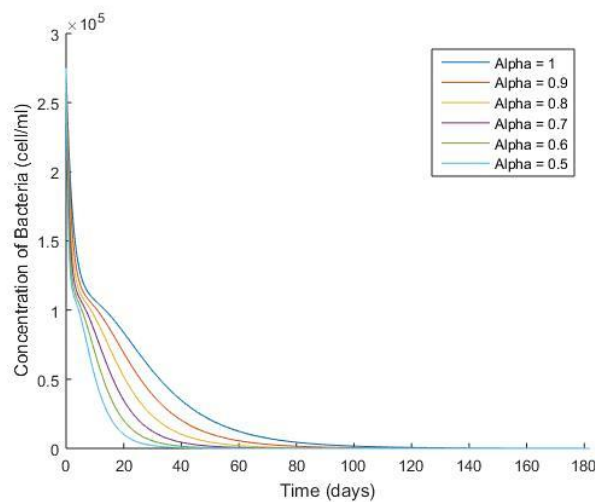
Figure 9. Simulations of the concentration of bacteria with different values of alpha.

6. Conclusion

This study investigates the use of fractional optimal control to mitigate cholera epidemics, emphasizing its potential to enhance the efficacy of intervention strategies. The key findings and outcomes are as follows:

- A system of fractional-order differential equations was formulated to accurately capture the dynamics of cholera spread.
- The mathematical analysis ensures the non-negativity and boundedness of solutions, confirming the ability of the model to accurately represent disease dynamics.
- Quarantine is incorporated as a control measure to reduce both the number of infected individuals and the bacterial concentration in the environment.
- Pontryagin's Maximum Principle is applied to derive optimal control strategies, ensuring the interventions are cost-effective and impactful.
- MATLAB-based simulations validate the effectiveness of the proposed control strategy, showing a significant reduction in the spread of disease and bacterial concentration.
- The basic reproduction number ($\mathcal{R}_0$) is computed using the next-generation matrix method.
- Stability analysis demonstrates the local asymptotic stability of both disease-free and endemic equilibrium points, highlighting the robustness of the model.
- Fractional calculus is successfully integrated into the control model, enhancing its precision and adaptability in cholera epidemic management.

7. Future directions

To build on the findings of this study, the following avenues can be explored:

- Extend the model to include vaccination, water sanitation, and public awareness campaigns alongside quarantine.
- Perform a detailed analysis of the economic and social costs associated with the interventions to assess their feasibility in resource-limited settings.

- Apply the model to real-world cholera outbreak data to validate its predictions and refine parameter estimates.
- Extend the model to account for spatial heterogeneity, enabling the study of cholera dynamics across interconnected regions.

By addressing these areas, the proposed framework can be further enhanced, providing a more comprehensive and practical approach to controlling cholera epidemics.

Author contributions: Conceptualization, BA and MH; methodology, BA; software, BA; validation, BA, MUR and MH; formal analysis, BA; investigation, BA; resources, BA; data curation, BA; writing—original draft preparation, BA; writing—review and editing, BA and MUR; visualization, BA; supervision, BA; project administration, MH; funding acquisition, BA and MUR. All authors have read and agreed to the published version of the manuscript.

Conflict of interest: The authors declare no conflict of interest.

References

1. Shuai Z, Tien JH, van den Driessche P. Cholera models with hyperinfectivity and temporary immunity. Bull. Math. Biol. 2012; 74: 2423–2445.
2. Penrose K, Castro MCD, Werema J, Ryan ET. Informal urban settlements and cholera risk in Dar es Salaam, Tanzania. PLoS Neglected Tropical Diseases. 2010; 4(3): e631.
3. Capasso V, Paveri-Fontana SL. A mathematical model for the 1973 cholera epidemic in the European Mediterranean region. Rev. Epidemiol. Sante Publique. 1979; 27(2): 121–132.
4. Codeço CT. Endemic and epidemic dynamics of cholera: The role of the aquatic reservoir. BMC Infectious Diseases. 2001; 1: 1–14.
5. Hartley DM, Morris Jr JG, Smith DL. Hyperinfectivity: A critical element in the ability of V. cholerae to cause epidemics? PLoS Medicine. 2006; 3(1): e7.
6. Mukandavire Z, Liao S, Wang J, et al. Estimating the reproductive numbers for the 2008–2009 cholera outbreaks in Zimbabwe. Proc. Natl. Acad. Sci. U. S. A. 2011; 108(21): 8767–8772.
7. Chen X, Sheng J, Wang X, Deng J. Exploring determinants of attraction and helpfulness of online product review: A consumer behaviour perspective. Discrete RMS: Research In Mathematics & Statistics 11 Dynamics in Nature and Society. 2016; 1–19.
8. Purnawan H, Faroh RA, Wahyudi MH, Cahyaningtias S. Optimal control with treatment and water sanitation for cholera epidemic model. EKSAKTA: Berkala Ilmiah Bidang MIPA. 2023; 23(03): 373–381.
9. Nisar, Kottakkaran Sooppy, Muhammad Farman, Mahmoud Abdel-Aty, and Jinde Cao. A review on epidemic models in sight of fractional calculus. Alexandria Engineering Journal. 2023; 75(2023): 81-113.
10. Cui X, Xue D, Pan F. A fractional SVIR-B epidemic model for Cholera with imperfect vaccination and saturated treatment. The European Physical Journal Plus. 2022; 137(12): 1361.
11. Allen L. An introduction to mathematical biology. Pearson; 2007.
12. Baba IA, Humphries UW, Rihan FA. A Well-Posed Fractional Order Cholera Model with Saturated Incidence Rate. Entropy. 2023; 25(2): 360.
13. Lemos-Paiao AP, Silva CJ, Torres DF. An epidemic model for cholera with optimal control treatment. Journal of Computational and Applied Mathematics. 2017; 318: 168–180.
14. Adom-Konadu A, Sackitey AL, Anokye M. Local Stability Analysis of epidemic models using a Corollary of Gershgorin's Circle Theorem. Research Square. 2022.
15. Khan MA, Islam S, Arif M, ul Haq Z. Transmission model of hepatitis B virus with the migration effect. BioMed Research International. 2013; 1: 150681.

16. Sweilam NH, AL-Mekhlafi SM, Baleanu D. Optimal control for a fractional tuberculosis infection model including the impact of diabetes and resistant strains. Journal of Advanced Research. 2019; 17: 125–137.

17. Index Mundi. Available online: http://www.indexmundi.com/g/g.aspx?c=ha&v=25 (accessed 25 December 2024).

18. Index Mundi. Available online: http://www.indexmundi.com/g/g.aspx?c=ha&v=26 (accessed 25 December 2024).

19. Capone F, De Cataldis V, De Luca R. Influence of diffusion on the stability of equilibria in a reaction–diffusion system modeling cholera dynamic. Journal of Mathematical Biology. 2015; 71: 1107–1131.

20. Sanches RP, Ferreira CP, Kraenkel RA. The role of immunity and seasonality in cholera epidemics. Bulletin of Mathematical Biology. 2011; 73: 2916–2931.

21. Neilan RLM, Schaefer E, Gaff H. Modeling optimal intervention strategies for cholera. Bulletin of Mathematical Biology. 2010; 72: 2004–2018.

22. Mwasa A, Tchuenche JM. Mathematical analysis of a cholera model with public health interventions. Biosystems. 2011; 105(3): 190–200.

23. World Health Organization. Global Task Force on Cholera Control, Cholera Country Profile: Haiti. Available online: https://geoconfluences.ens-lyon.fr/doc/transv/sante/popup/HaitiCountryProfileMay2011.pdf (accessed 25 December 2024).